Development of novel immunotherapy based on nanoparticle co-delivering PLK1 and PD-L1 inhibitors for lung cancer treatment

Moataz Reda
PDX Pharmaceuticals
Worapol Ngamcherdtrakul
PDX Pharmaceuticals
Natnaree Siriwon
University of Southern California
Daniel Bejan
PDX Pharmaceuticals
Sherif Reda
PDX Pharmaceuticals
Ruijie Wang
PDX Pharmaceuticals
Molly Nelson
PDX Pharmaceuticals
Husam Zaidan
PDX Pharmaceuticals
Ngoc Hoang
Oregon Health and Science University
Akash Bindal
Oregon Health and Science University
Gordon Mills
Oregon Health and Science University https://orcid.org/0000-0002-0144-9614
Joe Gray
Oregon Health and Science University https://orcid.org/0000-0001-9225-6756
Wassana Yantasee (yantasee@ohsu.edu)
Oregon Health and Science University

Article

Keywords: Immune Checkpoint Inhibitors, Volasertib, Mitotic Kinase, Abscopal Effect

DOI: https://doi.org/10.21203/rs.3.rs-142908/v1

Abstract

Immune checkpoint inhibitors (ICIs) targeting PD-L1 and PD-1 have improved survival in a subset of patients with advanced non-small cell lung cancer (NSCLC). However, only a minority of NSCLC patients respond to ICIs, highlighting the need for superior immunotherapy. Herein, we developed a nanoparticle-based immunotherapy termed ARAC (Antigen Release Agent and Checkpoint Inhibitor) to enhance the efficacy of PD-L1 inhibitor. ARAC is nanoparticle co-delivering PLK1 inhibitor, volasertib, and PD-L1 antibody. PLK1 is a key mitotic kinase that is overexpressed in various cancers including NSCLC and drives cancer growth. Inhibition of PLK1 selectively kills cancer cells and upregulates PD-L1 expression in surviving cancer cells thereby providing opportunity for ARAC targeted delivery in a positive feedback manner. ARAC reduced effective doses of volasertib and PD-L1 antibody by 5-fold in a metastatic lung tumor model and the effect was mainly mediated by CD8 + T cells. We also observed abscopal effect of ARAC in bilateral NSCLC tumor model and achieved complete cures in some mice when incorporating immune-stimulant CpG onto ARAC. Further, ARAC was well-tolerated in non-human primates. This study highlights a rationale combination strategy to augment existing therapies by utilizing our nanoparticle platform that can load multiple cargo types at once.

Introduction

The emergence of immune checkpoint inhibitors (ICIs) specifically antibodies targeting the PD-1/PD-L1 axis has reshaped the treatment landscape for various cancers including non-small cell lung cancer (NSCLC). PD-L1 expression on tumor cells inhibits tumor-directed cytotoxic CD8+ T cell activity by binding to PD-1 receptor on T cells and suppressing their function.[1-3] Thus, PD-1/PD-L1 overexpression is a hallmark of the immunosuppressive environment displayed in several types of cancer. PD-1/PD-L1 blockade induces potent responses in patients; however, only 15-20% of patients respond, and many initial responders often relapse suggesting resistance mechanisms.[4-6] PD-L1 expression has emerged as a biomarker to predict response to ICIs as high levels of PD-L1 are often associated with more responsive treatment outcomes,[7] while low levels of tumor infiltrating lymphocytes (TILs) are associated with lack of response or eventual resistance.[7,8] Thus, combinatorial strategies employing PD-L1/PD-1 inhibitors with other therapeutics that 1) upregulate PD-L1 expression and/or 2) increase density of TILs have great potential to enhance the response rate of treatments, and identify more curative approaches. Another limitation is that systemic distribution of ICIs can result in pathologic autoimmunity, leading to immune-related adverse events (irAEs) that damage normal tissues.[9] Therefore, combinatorial strategies to lower drug doses and improve safety have important clinical relevance.

Polo-like kinase 1 (PLK1) is a critical mitotic kinase that is overexpressed in various cancers and provokes oncogenic properties.[10] Previous studies have illustrated the potential of PLK1 inhibition as a strong therapeutic strategy and several PLK1 small molecule inhibitors have reached clinical trials.[11] However, clinical utility of PLK1 inhibitors has yet to be realized due to dose-limiting toxicities and poor efficacy as a monotherapy; thus, alternative therapeutic strategies are needed to elicit the full potential of

inhibiting PLK1. Herein, we investigate the relationship of PLK1 inhibition with immune checkpoint blockade. We report for the first time that PLK1 inhibition upregulates PD-L1 expression of cancer cells, thereby diminishing cytotoxic T cell function. Accordingly, the combination of PD-L1 blockade with PLK1 inhibition significantly reduced tumor burden and prolonged survival of lung tumor-bearing mice.

To facilitate clinical translation of this combination, we developed a nano-immunotherapy termed ARAC (Antigen Release Agent and Checkpoint inhibitor) for co-delivery of the PLK1 inhibitor (volasertib) and PD-L1 antibody. ARAC is built upon our polymeric modified mesoporous silica nanoparticle (NP) platform, which has shown substantial promise as a tumor-targeted delivery vehicle.[12] Indeed, we show that delivery of the therapeutic compounds (volasertib and PD-L1 antibody) with our NP platform can reduce the effective drug doses by 5-fold in a metastatic lung tumor model. This is significant as it alleviates toxicity concerns of each drug, while maintaining the therapeutic integrity of the drug combination. Volasertib induces cancer cell death and subsequent antigen release, while also upregulating PD-L1 expression of surviving cancer cells, providing the opportunity to target surviving cancer with PD-L1 antibody-conjugated nanoparticles (benefiting cancer otherwise having no obvious receptors for drug delivery). The upregulation of PD-L1 expression also renders cancer more responsive to PD-1/PD-L1 blockade with PD-L1 antibody on ARAC. Cellular uptake of ARAC by endocytosis in cancer cells leads to lower levels of membrane PD-L1 expression, allowing the cancer cells to be attacked by cytotoxic T cells. Our study provides evidence for the relationship between PLK1 inhibition and cancer immunosuppression and supports the combination of PLK1 inhibitor and PD-L1 immune checkpoint blockade as a potential therapeutic option. Further, our study highlights a rationale combination strategy to augment existing therapies without increasing toxicity by utilizing nanoparticle platform as a delivery carrier.

Results

PLK1 inhibition upregulates PD-L1 expression

We and others have previously reported that PLK1 inhibition or knock-down results in cell cycle arrest in G2/M leading to cancer cell death.[13-15] Herein, we found that PLK1 knockdown also results in an increase in PD-L1 surface expression in both human (A549) and murine (LLC-JSP) lung cancer cell lines. As shown in Fig. 1A, 85% knockdown of PLK1 mRNA (by siRNA against PLK1) resulted in 2.5-fold increase in PD-L1 mRNA expression in A549 cell line compared with scrambled siRNA (siSCR) treated cells. This was then confirmed at the surface protein level in A549 (Fig. 1B) and LLC-JSP (Fig. 1C) lung cancer cell lines at 3 days post siRNA treatments.

Mitotic kinase inhibitor (MKI)-induced PD-L1 expression

Following on the discovery that PLK1 inhibition results in PD-L1 upregulation, we sought to determine whether this holds true for inhibition of other mitotic kinases. We screened three leading mitotic kinase small molecule inhibitors against PLK1 (volasertib), Aurora kinase A (alisertib), and CHK1 (AZD7762) in human and mouse lung cancer cell lines. As shown in Supplementary Fig. 1, treatment of LLC-JSP (a

murine lung cancer cell line) with volasertib, alisertib, or AZD7762 led to significant cell death (Supplementary Fig. 1A) and upregulated surface PD-L1 level (Supplementary Figs. 1B&C) in each case. This not only establishes the link between mitotic kinase inhibition and PD-L1 upregulation, but also demonstrates the potency of volasertib over other mitotic kinase inhibitors.

Combination of PLK1 inhibition and PD-L1 blockade reduces tumor growth and prolongs survival in mice

Based on our finding that PLK1 inhibition upregulated PD-L1 protein, we aimed to investigate whether the PLK1 inhibitor volasertib and a PD-L1 monoclonal antibody would synergize *in vivo*. We used LLC-JSP cell line to develop a flank tumor model in immune-competent mice similar to previous report.[16] Mice with tumors (>60 mm^3) were treated i.p. with PLK1 inhibitor volasertib and PD-L1 antibody as shown in Fig. 2A. The combination treatment (volasertib + PD-L1 antibody) significantly reduced tumor growth (Fig. 2B) and prolonged survival of mice (Fig. 2C) compared to each monotherapy.

PD-L1 antibody conjugated nanoparticles for delivery of PLK1 inhibitor volasertib (ARAC)

Our data show for the first time the benefit of combining PD-L1 antibody and PLK1 inhibitor to enhance therapeutic impact. However, each drug alone carries significant toxicity risks which may limit the clinical translation of this combination. To overcome this limitation, we investigated a targeted delivery approach utilizing our polymer modified mesoporous silica nanoparticle (NP) platform. The same nanoparticle platform has been proven effective for targeted delivery of siRNA to breast tumors and lung tumors in our prior work.[12-14,17] Volasertib (iPLK1) was loaded onto mesoporous silica nanoparticle (MSNP) core prior to surface modification with polyethylenimine (PEI), polyethylene glycol (PEG), and PD-L1 antibody (Fig. 3A). The final composition contained 15% PEI and 13% PEG (by TGA), with 0.5% volasertib (by HPLC-UV-Vis), and 4.0% PD-L1 antibody (by BCA) (by weight of MSNP). Volasertib loaded nanoparticles, with PD-L1 antibody (p-iPLK1-NP; ARAC) and without (iPLK1-NP), had a size of 90 nm (Fig. 3B). As shown in Fig. 3C, treatment of LLC-JSP cells with iPLK1-NP significantly reduced cell viability more than the free volasertib counterpart given at the same dose. Similar results were obtained with B16-F10 melanoma cells and 4T1 breast cancer cells (Supplementary Fig. 2). In this case, PD-L1 antibody (see ARAC vs. iPLK1-NP; Fig. 3D) had no role in cancer killing (since there were no T cells in the system) or enhancing the delivery (since all nanoparticles were taken up by cells within 3 days regardless of having PD-L1 antibody or not). In agreement with previous finding using PLK1 siRNA (Fig. 1), treatment with iPLK1-NP resulted in significant increase in surface PD-L1 expression of the surviving cells at 2 days (about 60% cells were dead), but not at 2 hrs (Fig. 3E) since PLK1 inhibition effects (i.e. cell cycle arrest and death) had not yet transpired. However, PD-L1 antibody on the nanoparticles was as effective as free PD-L1 antibody, given at a 30-fold higher dose, at reducing surface PD-L1 level (see ARAC at 2 hrs, Fig. 3E). This is owing to the high local concentration of antibodies on the nanoparticles that the cells encountered. Nanoparticles with dense PD-L1 antibodies (approximately 2 x 10^3 antibodies per particle) bind multiple PD-L1 ligands on cell surface at once and are endocytosed with PD-L1 (termed receptor-meditated

endocytosis),[18] resulting in PD-L1 degradation (e.g., in lysosomes). Furthermore, Fig. 3E suggests that PD-L1 upregulation in the surviving population upon treatment with iPLK1-NP is not via selection process (e.g., death of cells with low PD-L1 first) since untreated cells (PBS) did not have a high PD-L1 population), but rather is due to signaling effects of PLK1 inhibition. Indeed, PLK1 inhibition also led to upregulation of PD-L1 expression in melanoma and breast cancer cells with varying PD-L1 baseline expression (Supplementary Fig. 2).

Feed-forward delivery and specificity of ARAC nanoconstruct

While ARAC initially reduces PD-L1 levels upon binding and internalization (as shown in Fig. 3E), surviving cells have upregulated PD-L1 due to the signaling effects of PLK1 inhibition. In this context, upregulated PD-L1 is used as the homing target for subsequent ARAC, leading to cancer targeting in a feedforward manner (i.e., higher targeting with increased doses of the treatment). To investigate the feedforward targeting of ARAC, we used 4T1 murine cancer cells which express low baseline PD-L1 levels. ARAC led to the upregulation of PD-L1 in 4T1 cells 4 days post treatment (Fig. 4A). We then assessed the cellular uptake of ARAC in control 4T1 cells (with low PD-L1) and ARAC-treated 4T1 cells (with upregulated PD-L1). As shown in Fig. 4B, after 1 hour of exposure, ARAC was preferentially taken up by the PD-L1 high cells vs. PD-L1 low cells by nearly 4-fold, demonstrating the selectivity and feed-forward targeting by ARAC. We also evaluated the cell killing selectivity by comparing viability of murine cancer cells (LLC-JSP, 4T1, B16-F10) vs. bone marrow-derived dendritic cells (BMDC) after treatment with ARAC. As shown in Fig. 4C, ARAC led to significant cell killing in cancer cells but minimal killing in dendritic cells. Similar to Fig. 3D, PD-L1 antibody has no effect on enhancing the delivery in this setting since all nanoparticles are taken up by cells within 3 days regardless of PD-L1 expression. Thus, the treatment selectivity to cancer cells over BMDC cells is due to cancer dependence on PLK1, as previously reported.[18]

ARAC induces systemic anti-tumor immune response in a bilateral lung cancer tumor model

To assess the anti-tumor immune response of ARAC, we utilized a bilateral flank tumor model. C57BL/6 mice were injected with 100K and 40K LLC-JSP cells on the right and left flank, respectively. At day 12 post injection, the right flank (local) tumors were injected with PBS, p-NP (NP with PD-L1 antibody), iPLK1-NP (NP with volasertib), or ARAC as shown in Fig. 5A. Growth of local (treated) and distant (untreated) tumors were monitored. Treatments with ARAC significantly reduced growth of local tumors compared with p-NP or iPLK1-NP (Fig. 5B). Importantly, a significant delay in the onset of distal tumors was also observed in ARAC group (Fig. 5C), suggesting that whole-body anti-tumor immune response was generated. Further, ARAC significantly prolonged survival of mice vs. saline or single drug NPs (Fig. 5D). In a separate study, mice were injected with saline or ARAC as shown in Fig. 5A and injected (local) tumors were harvested one day post last treatment to assess T cell infiltration. ARAC treated tumors had

significantly higher infiltrating lymphocytes (CD3+ T cells), specifically cytotoxic CD8+ T cells, than the control (Fig. 5E).

NP delivery reduces effective doses of PLK1 inhibitor and PD-L1 antibody in lung tumor mice by 5-fold

To evaluate ARAC systemically, we developed an experimental metastatic lung tumor model by intravenous injection of LLC-JSP cells (200K cells), which developed tumors mainly in the lungs (confirmed at sacrifice). Mice were randomly grouped and treated intravenously (i.v.) via tail vein with saline, free drugs (volasertib + PD-L1 antibody at same dose or 5-fold higher dose than dose on ARAC), ARAC, or ARAC plus anti-CD8 antibody (Fig. 6A). Mice treated with ARAC survived significantly longer than those treated with saline or free drugs at same dose (***$p<0.001$ vs. saline; **$p<0.01$ vs. free drugs (1x)) (Fig. 6B) and slightly better than those treated with the 5-fold dose of the free drug combo (*$p<0.05$ vs. saline). Thus, delivery with ARAC could effectively reduce required dose of drug by at least 5-fold. Moreover, ARAC's efficacy was confirmed to be immune-mediated as CD8+ T cell depletion by anti-CD8 antibodies abolished the prolonged survival of ARAC-treated mice (Fig. 6C). Furthermore, treatment with ARAC did not cause any weight loss, demonstrating its safety in mice (Fig. 6D).

Incorporating CpG adjuvant to ARAC (ARAC-CpG) enhances anti-tumor immune effects resulting in cures

We investigated whether the CpG adjuvant could further stimulate anti-tumor immunity and improve tumor control in a bilateral tumor model shown in Fig. 5. CpG 1826 (class B CpG for mice) was loaded on ARAC at 4% by weight of MSNP (complete loading confirmed by Nanodrop Spectrophotometer) with no significant change in hydrodynamic size (Fig. 7A). Both ARAC and ARAC-CpG significantly reduced tumor growth compared with saline-treated mice (Fig. 7B). Moreover, ARAC-CpG resulted in complete cure in 2 out of 7 mice (Fig. 7C), while no cures were achieved in ARAC-treated mice. CpG oligodeoxynucleotides act as a danger associated molecular pattern (DAMP) to stimulate pattern recognition receptors, specifically the toll-like receptor 9 (TLR9). This leads to the activation of antigen presenting cells and subsequent priming of T cells. Thus, by releasing antigens (via cancer killing by volasertib), delivering CpG adjuvant, and blocking PD-L1 immune checkpoints, ARAC-CpG tackles various strategies by which cancer cells evade the immune response; hence complete cures were achieved with this strategy.

Safety of nanoparticle platform in Cynomolgus monkeys

To date, we found our nanoparticle (NP) platform conjugated with trastuzumab (HER2 antibody) for delivering of HER2 siRNA to meet required safety criteria: (1) Low cytotoxicity of multiple organ cells (<10% cell death),[17] (2) Great blood compatibility,[12] (3) Not triggering adverse immune response of blood immune cells (PBMC),[12] (4) Excellent safety after 9 doses given to mice over 1 month by not causing

adverse effects to body weight, serum biomarkers, and histology of kidney and liver,[19] (5) Good maximum tolerated dose up to 5-fold of efficacious dose,[19] and (6) effective clearance as MSNP is soluble to benign silicic acid[20,21] at serum pH and cleared in urine.[19] Herein, we report preliminary toxicology study of nanoparticle platform co-delivering a PLK1 inhibitor (siRNA) and PD-L1 antibody (avelumab) in non-human primates (NHP), conducted by Charles River Lab (CRL). Avelumab (Merck/Pfizer) is an FDA approved PD-L1 antibody and was selected as the PD-L1 antibody as it has the highest binding affinity compared with other approved PD-L1 antibodies and also causes antibody-dependent cell cytotoxicity (ADCC) effects.[22] Cynomolgus monkeys (n=3) received intravenous infusion of 5.6 mg/kg bare NP, 6 mg/kg ARAC (estimated efficacious dose) and 18 mg/kg ARAC (3-fold efficacious dose), with a one week washout period in between dosing. Clinical signs, body weights, food consumption, dermal observations, clinical pathology parameters (hematology, coagulation, clinical chemistry, and cytokine secretion), gross necropsy findings, organ weights, and histopathologic examinations were evaluated. There were no test article-related clinical observations or effects on body weight (Supplementary Table 1), food consumption, or coagulation (Supplementary Table 3). Dermal observations of erythema and edema were noted at 6 and 24 hours post dose but resolved at 48 hrs post dose (Supplementary Table 6). For hematology, nonadverse decreased white blood cell (WBC), neutrophil, and lymphocyte counts were observed in 2 of 3 monkeys at the highest dose (18 mg/kg ARAC) on day 2 post dose but were resolved by day 7 post dose, indicating recovery (Table 1; Supplementary Table 2). For clinical chemistry, nonadverse increased aspartate aminotransferase (AST) and alanine aminotransferase (ALT) levels were noted on day 2 following administration of NP alone, 6 mg/kg ARAC, and 18 mg/kg ARAC. However, for each group, AST and ALT levels of day 7 were similar to predose values, indicating recovery (Table 1; Supplementary Table 4). Further, key cytokines (IL-1b, IL-6, IFN-g, TNF-a, IFN-a, and MCP-1) were monitored in serum collected at 0, 6, 24, and 48 hours. Even in monkeys receiving the highest dose (18 mg/kg), only MCP-1 and IFN-a were mildly to moderately elevated in 2 out of 3 monkeys at 6 hrs, which subsided at 24 hrs without intervention (Supplementary Table 5). Increase of these cytokines right after treatment may be part of therapeutic actions (e.g., IFN-a suggests induction of innate immunity by siRNA;[23,24] PD-L1 inhibition induced a higher production of MCP-1).[25] Terminal euthanasia and necropsy was performed one week following the 18 mg/kg dosing to assess gross pathology, organ weights, and histopathology. A few observations were noted that were considered incidental and of the nature commonly observed in this species and age of monkeys. Thus, there were no test article-related effects on survival, organ weights, gross pathology, or histopathology (Supplementary Tables 7-9). In conclusion, the nanoconstruct was found to be safe and well tolerated in NHP at up to 3-fold anticipated efficacious dose. Based on these results, the no-observed-adverse-effect level (NOAEL) for ARAC was considered to be 18 mg/kg. Dose-limiting toxicity (DLT) of ARAC was not reached in this preliminary study and will be determined in subsequent NHP studies.

Discussion

The potential of PLK1 inhibition as a therapeutic strategy has been well studied in various cancer types; however, the interplay of PLK1 inhibition with cancer immunity remains mostly unexplored. In this study,

we report for the first time that PLK1 inhibition results in an increase of immune checkpoint PD-L1 expression in cancer cells. This suggests that evading the immune response is a mechanism exploited by cancer cells that survive PLK1 inhibition. Consequently, we show that the combination of PLK1 inhibitor and PD-L1 antibody significantly reduced tumor progression in mice compared to each drug alone. In addition to its well-studied mitotic functions, recent studies have highlighted the role of PLK1 in immune regulation in several types of cancer.[26] Notably, PLK1 expression has been shown to inhibit immune cell infiltration and anti-tumor immunity. In regards to NSCLC subtypes (lung squamous cell carcinoma and lung adenocarcinoma), PLK1 expression is negatively correlated with immune scores, major histocompatibility complex (MHC) class I activity, and gene expression of TILs.[26] Furthermore, PLK1 expression has been shown to be an activator of STAT3, which promotes an immunosuppressive environment.[26] In addition, PLK1 was found to associate with mitochondrial anti-viral signaling (MAVS) protein to negatively control its activity in inducing type I interferons.[27] Collectively, these data suggest that increased expression of PLK1 in several types of cancer, including NSCLC, may contribute to the immunosuppressive tumor microenvironment (TME). Thus, targeting PLK1 may provide a therapeutic strategy to enhance anti-tumor immunity. Indeed, inhibition of PLK1 results in reduced phosphorylation of STAT3,[14,27] thereby dampening its activity in NSCLC cells. Furthermore, PLK1 inhibition has been shown to increase MHC Class I expression on multiple cell lines,[26] suggesting a role in adaptive immunity. Taken together, such observations suggest that elevated levels of PLK1 not only contribute to cancer cell division and proliferation, but may play a significant role in the aberrant immune function of cancer. More importantly, this suggests that PLK1 inhibition may be promising way to augment immunotherapy. However, to the best of our knowledge, this is the first study to report the effectiveness of the combination of PLK1 inhibition with any immunotherapy.

To overcome the dose limiting toxicity of current PLK1 inhibitors that prevent them from advancing beyond clinical trials, we developed a PLK1 inhibitor loaded nanoparticle platform and conjugated it to PD-L1 antibody (ARAC) to synergize combination effects of PLK1 inhibition and PD-L1 blockade. In our prior works, we reported on the efficacy and safety profile of this nanoparticle platform in delivering siRNA to mediate gene knockdown of breast and lung tumors *in vivo.*[12,14] In this research, we demonstrate that the platform can also improve delivery of small molecule inhibitors (i.e. volasertib) as treatment with PLK1 inhibitor on nanoparticles significantly reduced cell viability compared with free PLK1 inhibitor. In mice bearing bilateral tumors, 3 doses of intratumoral ARAC reduced growth of local (injected) tumors compared with nanoparticle delivering a single drug, and delayed the onset of distant tumors suggesting that a whole-body anti-tumor response was triggered. Further, the therapeutic benefit of nanoparticle delivery was demonstrated in an experimental metastatic lung tumor model, where i.v. administration of ARAC improved survival as much as the free drugs at 5-fold higher dose. This suggests that nanoparticle delivery can overcome dose limiting toxicity issues of PLK1 inhibitors and thereby facilitate clinical utility. ARAC's efficacy was confirmed to be immune-mediated as CD8 depletion abolished the prolonged survival. Importantly, i.v. administration of the nanoparticle platform was found to be well tolerated and safe to Cynomolgus monkeys at up to 3-fold estimated efficacious dose in a preliminary toxicology study.

Mechanistically, ARAC leads to cell cycle arrest and generation of an anti-tumor immune response, while exhibiting unique feed-forward delivery capability (e.g., greater delivery to surviving cancer cells having upregulated PD-L1 levels from an initial treatment) to mount an anti-tumor immune attack (Scheme 1). For tumors with initially low PD-L1 levels, ARAC with slight positive charge (6 mV in 10 mM NaCl) may rely first on enhanced permeability and retention effect (EPR) and adsorptive endocytosis and subsequently on PD-L1 antibody mediated endocytosis after volasertib-induced PD-L1 upregulation in the surviving cancer cells. While toxic to multiple cancer cell types, ARAC is safe to antigen-presenting cells (DCs), needed for generating anti-tumor T cells. Incorporating CpG, to enhance DC activation and T cell priming, into ARAC led to complete cures for some mice in bilateral tumor model. This is owing to the versatility of the nanoparticle platform that can load multiple therapeutic compounds at once without increasing hydrodynamic particle size. For application to lung cancer, systemic ARAC-CpG will be further investigated in lung tumor models and will be compared with systemic ARAC plus subcutaneous CpG (a more preferred route of CpG) in due course.[28]

Our research herein focused on lung cancer, the leading cancer killer.[29] Like melanoma, where immunotherapy has been the most promising, lung cancer is a disease with a high mutational load which drives the expression of various neo-epitopes which can be recognized by host immune system.[30,31] Consequently, immunotherapy is a promising approach to treat lung cancer. However, objective response rates are much lower for lung cancer patients than melanoma. The research described here illustrates how superior responses can be achieved for lung cancers when combining PLK1 inhibition with PD-L1 blockade. Further, other cytotoxic agents have also been shown to increase PD-L1 expression, including paclitaxel in ovarian cancer,[32] CDK4/6 inhibitors,[33] and PARP inhibitors[34] in breast cancer. Therefore, it is logical that these drugs are now in clinical investigations in combination with PD-1/PD-L1 checkpoint blockade.[35] Our findings suggest that co-delivering these drugs with PD-L1 immune checkpoint antibody on our nanoparticles will increase efficacy while lowering toxicity. Further, as PLK1 overexpression has been found in a variety of cancers, the combination of PLK1 inhibition and PD-L1 blockade may have broad application to a plethora of cancers. Lastly, other mitotic kinase inhibitors which will elevate PD-L1 expression of cancer cells should also be combined with PD-L1 immune checkpoint blockade to improve treatment outcomes in clinics.

Methods

Cell lines and reagents

A549 NSCLC were purchased from ATCC (CCL-185) and maintained in RPMI media with 10% fetal bovine serum (FBS). Lewis Lung Carcinoma (LLC) metastatic variant, LLC-JSP cells were gift from Dr. Don Gibbons lab (MD Anderson Cancer Center), and were cultured in RPMI + 10% FBS. BMDCs were harvested from Balb/c mice and cultured following published protocols.[36,37] Antibodies used: Human PD-L1 antibody (eBioscience), mouse PD-L1 (PE, BD Biosciences), mouse CD3 (APC, eBioscience), mouse CD8a

(Pacific Blue, Invitrogen), mouse CD4 (BV711, BD biosciences), mouse PD-1 (PE/Cy7, BioLegend). Alexa Fluor 488 secondary antibody was purchased from Life Technologies. *In vivo* grade mouse PD-L1 antibody (BE0101) and mouse CD8 antibody were purchased from BioXcell, and volasertib was purchased from Selleckchem. Pharmaceutical-grade human PD-L1 antibody avelumab was purchased from OHSU Pharmacy. SiRNA sequences: PLK1 (antisense 5'-UAUUCAUUCUUCUUGAUCCGG-3'); scrambled SCR (antisense 5'-UUAGUCGACAUGUAAACCA-3') were purchased from Dharmacon. CpG 1826 (sequence: 5'-tccatgacgttcctgacgtt-3') was purchased from Invivogen.

Nanoparticle synthesis and characterization

Bare MSNPs were synthesized as we have previously reported.[12] For PLK1 inhibitor loading, volasertib was dissolved in DMSO and diluted in ethanol solution and mixed with MSNPs in ethanol for overnight shaking at room temperature (350 RPM). The next day, nanoparticles were coated with 10 kDa branched PEI (Alfa Aesar) and 5 kDa mal-PEG-NHS (Jenkem) following our previous studies.[12,38] For PD-L1 antibody conjugation, *in vivo* grade mouse PD-L1 antibody (BioXcell) or avelumab was buffer exchanged to PBS pH 8 (Zeba spin column, Thermo Fisher) and thiolated using Traut's reagent (Thermo Fisher) following manufacturer's protocol. Thiolated antibody was added to NP at 20 wt.% and shaken overnight at 4^{o}C (300 RPM). Nanoparticles were washed with PBS pH 7.2 before characterization. Nanoparticle size was 90 nm, determined using Malvern Zetasizer. Antibody loading was 4 wt.%, determined by protein quantification of NP supernatant with BCA assay. To quantify PLK1 inhibitor loading, nanoparticles were shaken in DMSO solution to release the drug and supernatant was collected. Absorbance of supernatant was measured with Tecan plate reader to determine loading extent to be 0.5 wt.%. CpG oligo or siRNA was loaded onto the nanoparticles by 5-min mixing in PBS at room temperature, and complete loading was confirmed by Nanodrop Spectrophotometer. ARAC refers to nanoparticle loaded with both PLK1 inhibitor and PD-L1 antibody, p-NP is nanoparticle loaded with PD-L1 antibody, and iPLK1-NP is nanoparticle loaded with PLK1 inhibitor.

Flow cytometry

Cells (100K cells/well) were plated in 6 well plates overnight and treated with indicated treatments the next day. Following treatments, cells were collected and aliquoted to 1 million cells per sample before washing in FACs buffer and staining. Primary and secondary antibodies were stained for 30 mins and 1 hour, respectively, under rocking on ice. After staining, cells were washed in FACs buffer before flow analysis with Guava easyCyte (Millipore Sigma) flow cytometer (10,000 events per sample). For tumor immune profiling, tumors were harvested, minced, and incubated with 1 mg/ml DNAse for 30 minutes before smashing through 70 µm filter to obtain single cell suspension. RBC lysis buffer was incubated with cells for 5 minutes, and washed with PBS. 1 million cells per sample were blocked with Fc-shield before staining with dye conjugated antibodies for 30 minutes (in FACs buffer). Cells were then washed with FACs buffer and analyzed with flow cytometry(50,000 events per sample).

Cell viability after treatments

Cells (1500/well) were plated in white flat bottom 96 well plate overnight. The following day, cells were treated with drug loaded nanoparticles and controls as indicated and media was changed 24 hr post treatment. 3-5 day post treatment, cell viability was assessed using Cell Titer Glo assay (Promega) following manufacturer's instructions. Luminescence was read with Tecan plate reader.

RT-qPCR to assess PLK1 and PD-L1 mRNA

RNA was isolated with GeneJet RNA purification kit (Thermo Fisher Scientific) following manufacturer's instructions. One-Step qRT-PCR was performed using EXPRESS One-Step Superscript™ qRT-PCR Kit (Invitrogen). Cycling conditions: 50 ^{o}C for 2 min, 95 ^{o}C for 10 min, 40 cycles of 95 ^{o}C for 15 s, and 60 ^{o}C for 1 min. TAQMAN gene expression primers Human *HPRT* mRNA (Hs99999909_m1), Human *PLK1* mRNA (Hs00983225_g1), and Human PDL1 (Hs00204257_m1) were used. Data was analyzed using $2^{-\Delta\Delta C(t)}$ method.

Syngeneic tumor models and treatments

For single tumor flank model, LLC-JSP murine lung cancer cells (200K) were inoculated in right flank of C57BL/6 female mice (6 weeks) (Charles River NCI colony). At 8 days post tumor inoculation, mice received intraperitoneal (i.p.) treatments of volasertib (20 mg/kg) and/or PD-L1 antibody (10 mg/kg) every 5 days for 3 doses total. Tumors were measured with Vernier Caliper and volume calculated by V = 0.5 x length x width^2. For bilateral tumors, C57BL/6 were inoculated with 100K and 40K LLC-JSP cells in right and left flank, respectively. At 12 days post inoculation, the aforementioned treatments were administered intratumorally to the right tumor every 3 days for 3 doses total. For both single flank and bilateral flank tumor models, mice were sacrificed when total tumor burden exceeded 2000 mm^3. For metastatic lung tumor model, LLC-JSP (200K) were injected intravenously (i.v.) to 6 week old C57BL/6 mice. At 3 days post cancer cell injection, mice were randomly grouped and treated with i.v. saline, ARAC (25 mg/kg NP), ARAC plus CD8 antibody, or i.p. PD-L1 antibody (5 mg/kg) plus volasertib (1.25 mg/kg) every 3 days for a total of 4 doses. All studies were reviewed and approved by Institutional Animal Care and Use Committee (IACUC) at Oregon Health and Science University (OHSU).

Statistical analysis

GraphPad Prism 8.0 (GraphPad Software Inc.) was used for all statistical analysis. Comparison between two groups was performed with Student's *t* test. Tumor growth was analyzed using two-way repeated measures ANOVA with Tukey's correction for multiple comparisons. Kaplan Meier survival curve was analyzed using the log-rank (Mantel-Cox) method. Significance was set at $p < 0.05$. *In vitro* data are expressed as mean ± SD; *in vivo* data are expressed as mean ± SEM.

Declarations

Acknowledgement

This work was funded by the Wayne D. Kuni & Joan E. Kuni Foundation, NIH/NCI grant# R44CA217534, NIH/NCATS grant# R43TR001906, OHSU Knight Cancer Institute's Hillcrest Committee Pilot Award, and OHSU Center for Women's Health Circle of Giving Award. Its contents are solely the responsibility of the authors and do not necessarily represent the official views of the NIH. We thank Dr. Sudarshan Anand of OHSU's Cell, Developmental and Cancer Biology department for his independent review of the data as required by OHSU's conflict of interest guidelines. We thank Dr. Don Gibbons lab at MD Anderson Cancer Center for generous gift of LLC-JSP murine lung cancer cell line. Thanks to Drs. Michael Templin and Melinda Tyner at Charles River Laboratory (Ashland, Ohio) and their team for their assistance in designing and executing NHP studies along with data interpretation.

Conflict of Interest

OHSU, JWG, and WY have a significant financial interest in PDX Pharmaceuticals, Inc., a company that may have a commercial interest in the results of this research and technology. This potential personal and institutional conflict of interest has been reviewed and managed by OHSU.

References

1. Ohaegbulam KC, Assal A, Lazar-Molnar E, Yao Y, Zang X. Human cancer immunotherapy with antibodies to the PD-1 and PD-L1 pathway. *Trends in molecular medicine* 2015; **21**(1): 24-33.
2. Shrimali RK, Janik JE, Abu-Eid R, Mkrtichyan M, Khleif SN. Programmed death-1 & its ligands: promising targets for cancer immunotherapy. *Immunotherapy* 2015; **7**(7): 777-92.
3. Zou W, Wolchok JD, Chen L. PD-L1 (B7-H1) and PD-1 pathway blockade for cancer therapy: Mechanisms, response biomarkers, and combinations. *Science Translational Medicine* 2016; **8**(328): 328rv4-rv4.
4. Reck M, Rodríguez-Abreu D, Robinson AG, et al. Pembrolizumab versus Chemotherapy for PD-L1–Positive Non–Small-Cell Lung Cancer. *New England Journal of Medicine* 2016; **375**(19): 1823-33.
5. Malhotra J, Jabbour SK, Aisner J. Current state of immunotherapy for non-small cell lung cancer. *Translational lung cancer research* 2017; **6**(2): 196-211.
6. Moya-Horno I, Viteri S, Karachaliou N, Rosell R. Combination of immunotherapy with targeted therapies in advanced non-small cell lung cancer (NSCLC). *Therapeutic advances in medical oncology* 2018; **10**: 1758834017745012-.
7. Teng MWL, Ngiow SF, Ribas A, Smyth MJ. Classifying Cancers Based on T-cell Infiltration and PD-L1. *Cancer research* 2015; **75**(11): 2139-45.
8. Zhuang Y, Liu C, Liu J, Li G. Resistance Mechanism of PD-1/PD-L1 Blockade in the Cancer-Immunity Cycle. *Onco Targets Ther* 2020; **13**: 83-94.
9. Reynolds KL, Cohen JV, Ryan DP, et al. Severe immune-related adverse effects (irAE) requiring hospital admission in patients treated with immune checkpoint inhibitors for advanced malignancy:

Temporal trends and clinical significance. *Journal of Clinical Oncology* 2018; **36**(15_suppl): 3096-.

10. Liu Z, Sun Q, Wang X. PLK1, A Potential Target for Cancer Therapy. *Translational oncology* 2016; **10**(1): 22-32.
11. Gutteridge REA, Ndiaye MA, Liu X, Ahmad N. Plk1 Inhibitors in Cancer Therapy: From Laboratory to Clinics. *Molecular cancer therapeutics* 2016; **15**(7): 1427-35.
12. Ngamcherdtrakul W, Morry J, Gu S, et al. Cationic Polymer Modified Mesoporous Silica Nanoparticles for Targeted siRNA Delivery to HER2+ Breast Cancer. *Advanced Functional Materials* 2015; **25**(18): 2646-59.
13. Morry J, Ngamcherdtrakul W, Gu S, et al. Targeted treatment of metastatic breast cancer by PLK1 siRNA delivered by an antioxidant nanoparticle platform. *Molecular cancer therapeutics* 2017: DOI: 10.1158/535-7163.mct-16-0644.
14. Reda M, Ngamcherdtrakul W, Gu S, et al. PLK1 and EGFR targeted nanoparticle as a radiation sensitizer for non-small cell lung cancer. *Cancer Lett* 2019; **467**: 9-18.
15. McCarroll JA, Dwarte T, Baigude H, et al. Therapeutic targeting of polo-like kinase 1 using RNA-interfering nanoparticles (iNOPs) for the treatment of non-small cell lung cancer. *Oncotarget* 2015; **6**(14): 12020-34.
16. Chen L, Gibbons DL, Goswami S, et al. Metastasis is regulated via microRNA-200/ZEB1 axis control of tumour cell PD-L1 expression and intratumoral immunosuppression. *Nat Commun* 2014; **5**: 5241.
17. Gu S, Hu Z, Ngamcherdtrakul W, et al. Therapeutic siRNA for drug-resistant HER2-positive breast cancer. *Oncotarget* 2016; **7**(12): 14727-41.
18. Liu X, Lei M, Erikson RL. Normal cells, but not cancer cells, survive severe Plk1 depletion. *Mol Cell Biol* 2006; **26**(6): 2093-108.
19. Yantasee W, Gray JW, Ngamcherdtrakul W. Novel siRNA-nanoparticle platform for treating drug resistant HER2 positive breast cancer. Final Report to the National Cancer Institute (NCI) for the Phase II SBIR Contract # HHSN261201300078C to PDX Pharmaceuticals in collaboration with the BME of OHSU; September 9, 2016.
20. Ehlerding EB, Chen F, Cai W. Biodegradable and Renal Clearable Inorganic Nanoparticles. *Advanced science (Weinheim, Baden-Wurttemberg, Germany)* 2016; **3**(2).
21. Kempen PJ, Greasley S, Parker KA, et al. Theranostic Mesoporous Silica Nanoparticles Biodegrade after Pro-Survival Drug Delivery and Ultrasound/Magnetic Resonance Imaging of Stem Cells. *Theranostics* 2015; **5**(6): 631-42.
22. Akinleye A, Rasool Z. Immune checkpoint inhibitors of PD-L1 as cancer therapeutics. *J Hematol Oncol* 2019; **12**(1): 92-.
23. Judge AD, Sood V, Shaw JR, Fang D, McClintock K, MacLachlan I. Sequence-dependent stimulation of the mammalian innate immune response by synthetic siRNA. *Nature Biotechnology* 2005; **23**(4): 457-62.

24. Robbins M, Judge A, MacLachlan I. siRNA and innate immunity. *Oligonucleotides* 2009; **19**(2): 89-102.
25. Pei X, Fan X, Zhang H, et al. Low frequency, weak MCP-1 secretion and exhausted immune status of peripheral monocytes were associated with progression of severe enterovirus A71-infected hand, foot and mouth disease. *Clin Exp Immunol* 2019; **196**(3): 353-63.
26. Li M, Liu Z, Wang X. Exploration of the Combination of PLK1 Inhibition with Immunotherapy in Cancer Treatment. *Journal of oncology* 2018; **2018**: 3979527-.
27. Vitour D, Dabo S, Ahmadi Pour M, et al. Polo-like kinase 1 (PLK1) regulates interferon (IFN) induction by MAVS. *The Journal of biological chemistry* 2009; **284**(33): 21797-809.
28. Lou Y, Liu C, Lizée G, et al. Antitumor activity mediated by CpG: the route of administration is critical. *J Immunother* 2011; **34**(3): 279-88.
29. American Cancer Society. Cancer Facts & Figures. 2018.
30. Campbell JD, Alexandrov A, Kim J, et al. Distinct patterns of somatic genome alterations in lung adenocarcinomas and squamous cell carcinomas. *Nature genetics* 2016; **48**(6): 607-16.
31. Rizvi NA, Hellmann MD, Snyder A, et al. Mutational landscape determines sensitivity to PD-1 blockade in non–small cell lung cancer. *Science (New York, NY)* 2015; **348**(6230): 124-8.
32. Peng J, Hamanishi J, Matsumura N, et al. Chemotherapy Induces Programmed Cell Death-Ligand 1 Overexpression via the Nuclear Factor-kappaB to Foster an Immunosuppressive Tumor Microenvironment in Ovarian Cancer. *Cancer research* 2015; **75**(23): 5034-45.
33. Zhang J, Bu X, Wang H, et al. Cyclin D-CDK4 kinase destabilizes PD-L1 via cullin 3-SPOP to control cancer immune surveillance. *Nature* 2018; **553**(7686): 91-5.
34. Jiao S, Xia W, Yamaguchi H, et al. PARP Inhibitor Upregulates PD-L1 Expression and Enhances Cancer-Associated Immunosuppression. *Clin Cancer Res* 2017; **23**(14): 3711-20.
35. Esteva FJ, Hubbard-Lucey VM, Tang J, Pusztai L. Immunotherapy and targeted therapy combinations in metastatic breast cancer. *The Lancet Oncology* 2019; **20**(3): e175-e86.
36. Matheu MP, Sen D, Cahalan MD, Parker I. Generation of bone marrow derived murine dendritic cells for use in 2-photon imaging. *J Vis Exp* 2008; (17): 773.
37. Kimura A, Naka T, Kishimoto T. IL-6-dependent and -independent pathways in the development of interleukin 17-producing T helper cells. *Proceedings of the National Academy of Sciences* 2007; **104**(29): 12099.
38. Ngamcherdtrakul W, Sangvanich T, Reda M, Gu S, Bejan D, Yantasee W. Lyophilization and stability of antibody-conjugated mesoporous silica nanoparticle with cationic polymer and PEG for siRNA delivery. *Int J Nanomedicine* 2018; **13**: 4015-27.

Table And Scheme

Table 1 and Scheme 1 are available in the Supplementary Files

Figures

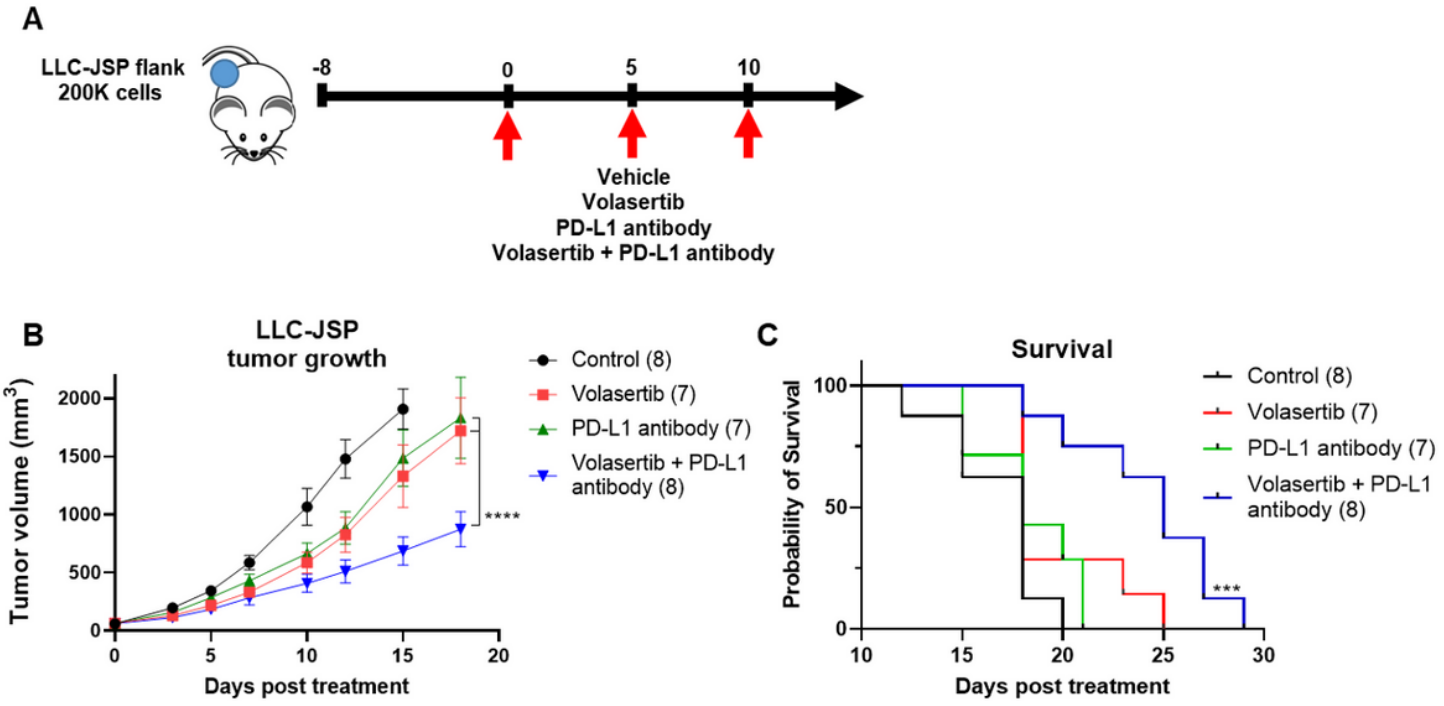

Figure 2

PLK1 inhibition potentiates PD-L1 blockade in syngeneic lung tumors. (A) C57BL/6 mice were injected with 200K LLC-JSP cells in right flank. On day 0 (8 post tumor inoculation), mice were grouped (n=7-8) and received i.p. treatments of control vehicles (PBS and HCl/saline), PLK1 inhibitor volasertib (20 mg/kg), PD-L1 antibody (10 mg/kg), or combination of PLK1 inhibitor and PD-L1 antibody at the same dose. Treatments were administered every 5 days for 3 doses. (B) Tumor growth of mice. Data presented as mean ± SEM; ***P<0.001, ****P<0.0001. (C) Kaplan-Meier Survival curve. ***P<0.001 vs. saline.

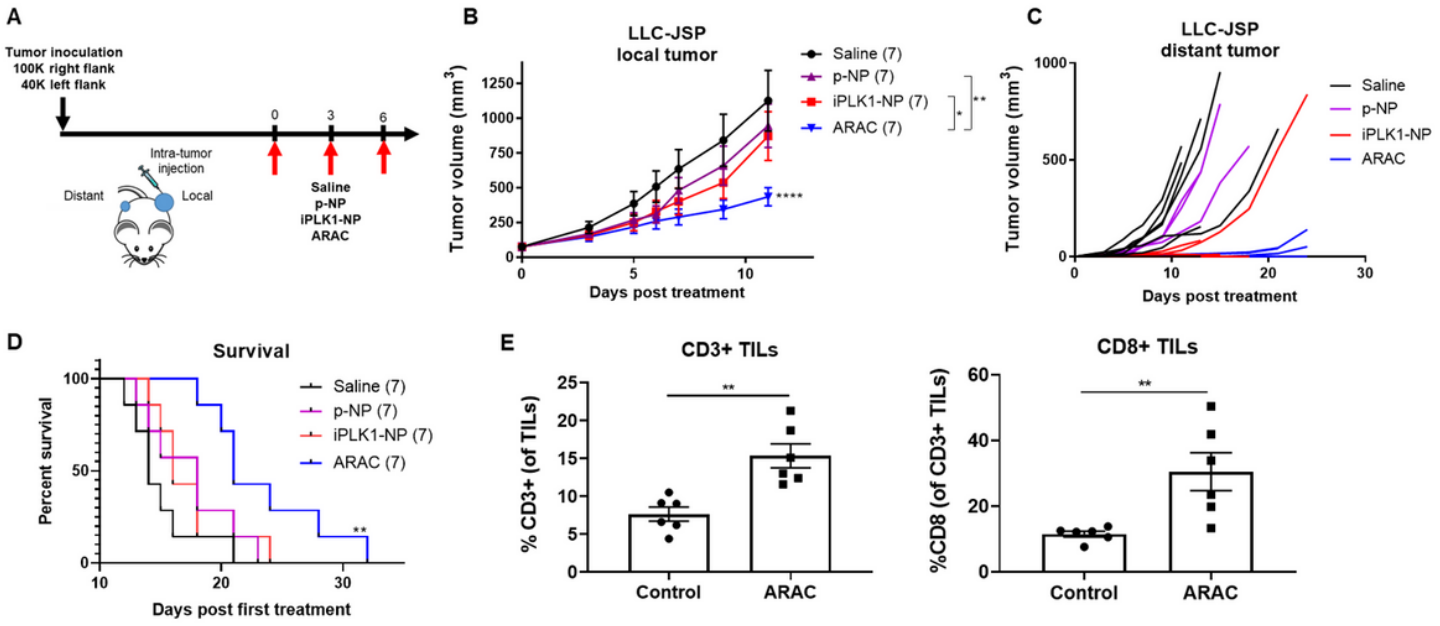

Figure 5

ARAC elicits anti-tumor immune effects. (A) 100K LLC-JSP cells were injected in right flank and 40K cells were injected in left flank of C57BL/6 mice. On day 12 post tumor inoculation, mice received intratumoral treatments of saline, p-NP, iPLK1-NP, or ARAC to the right (local) tumor. 0.5 mg NP (containing 2.5 µg volasertib and/or 20 µg PD-L1 antibody) in 50 µl per dose for 3 doses total. (B) Local tumor growth. (C) Distant (untreated) tumor growth of individual mice. (D) Kaplan Meier Survival curve (mice were euthanized when a combined tumor size reached 2000 mm3). (E) Mice were injected with tumors as described in (A) Tumor infiltrating lymphocytes (TILs) by flow cytometry (50,000 events per sample). Data presented as mean ± SEM; *P<0.05, **P<0.01, ****P<0.0001.

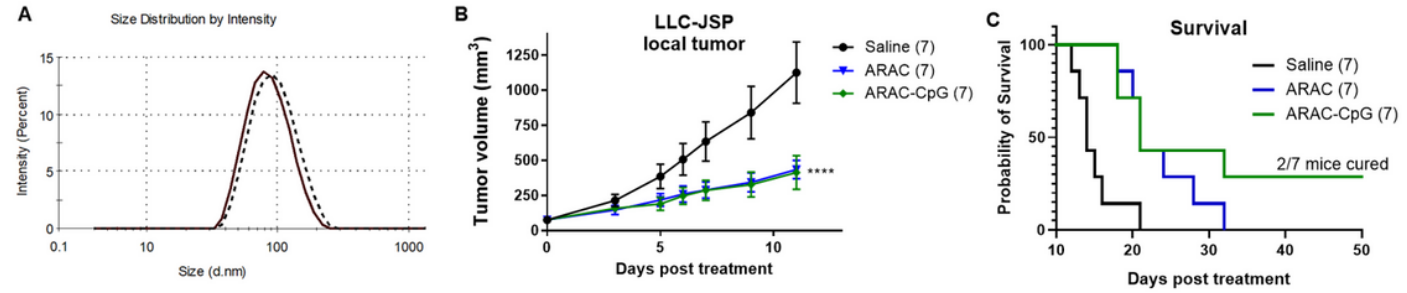

Figure 7

Adding CpG to ARAC (ARAC-CpG) enhances therapeutic benefit. CpG was loaded on ARAC (via electrostatic interaction with PEI) at 4% by weight of MSNP. (A) Hydrodynamic size of ARAC (solid) and ARAC-CpG (dotted). Following schedule in Fig. 5A, mice (n=7) received intratumoral treatments of ARAC-CpG to the right (local) tumor. 0.5 mg NP (2.5 µg iPLK1, 20 µg PD-L1 antibody, 20 µg CpG) in 50 µl. (B)

Local tumor growth of saline, ARAC, and ARAC-CpG. Data presented as mean ± SEM; ****P<0.0001 between ARAC-CpG and saline. (C) Kaplan Meier Survival curve.

Supplementary Files

This is a list of supplementary files associated with this preprint. Click to download.

- Table1.png